iJRASET
International Journal For Research in Applied Science and Engineering Technology

INTERNATIONAL JOURNAL FOR RESEARCH

IN APPLIED SCIENCE & ENGINEERING TECHNOLOGY

Volume: 4 **Issue:** IV **Month of publication:** April 2016

DOI:

www.ijraset.com

Call: 08813907089 | E-mail ID: ijraset@gmail.com

Volume 4 Issue IV, April 2016
ISSN: 2321-9653
International Journal for Research in Applied Science & Engineering Technology (IJRASET)

MnO_2, Co_3O_4 and MnO_2:Co_3O_4 Stacked Thin Film Electrodes for Supercapacitor

Dattatraya Sutrave[1], Sangeeta Jogade[2], Sriniwas Gothe[3]
[1,2]*D. B. F. Dayanand College of Arts and Science, Solapur, Maharashtra 413003*
[3]*Sangameshwar College, Solapur, Maharashtra 413003*

Abstract- ***In the present work, MnO_2, Co_3O_4 and MnO_2:Co_3O_4 stacked thin films were prepared by Sol-gel spin coat method with Manganese acetate and Cobalt acetate as precursors. The XRD patterns showed crystalline behaviour with orthorhombic and cubic phase for MnO_2 and Co_3O_4 respectively. MnO_2: Co_3O_4 stacked film showed dominating peaks of both oxides with two new peaks of MnO_2 and small shift in angle 2θ affecting lattice constants. The SEM images of MnO_2 and Co_3O_4 thin film revealed the formation of well adherent and porous tetragonal structure with apparent breadth in the range of 500nm to 600nm respectively. Whereas stacked film exhibited decreased grain size to around 250nm with improved porosity. From electrochemical analysis it is found that, the MnO_2, Co_3O_4 and MnO_2:Co_3O_4 stacked films showed maximum specific capacitance of 440 F/g, 530 F/g and 600 F/g respectively at 10mV/s scan rate in 0.1M KOH electrolyte, specific energy 20.13 Wh/kg, 72.22 Wh/kg and 141.66 Wh/kg respectively and specific power 29.00 KW/kg, 52.00 KW/kg, 68.00 KW/kg respectively. Furthermore 75% stability is retained after 1000 cycles exhibiting good cyclic stability and long cycle life. These results suggest that, MnO_2:Co_3O_4 stacked thin film can be a good electrode material for supercapacitor.***

Index Terms- ***CV, Co_3O_4, EIS, MnO_2, Sol-gel, Specific capacitance, Stability, Stacked oxide,***

I. INTRODUCTION

Nanocomposite thin films are formed by mixing two or more dissimilar materials having nano-dimensional phase(s) in order to control and develop new and improved structures and properties. The properties of nanocomposite films depend not only upon the individual components used but also on the morphology and the interfacial characteristics. Recently, various nanocomposite films consisting of either metal-metal oxide, mixed metal oxides, polymers mixed with metals or metal oxides, or carbon nanotubes mixed with polymers, metals or metal oxides have been synthesized and investigated for their application as active materials for supercapacitors. Design of the nanocomposite films for such applications needs the considerations of many factors, for example, the surface area, interfacial characteristics, electrical conductivity, nanocrystallite size, surface and interfacial energy, etc., all of which depend significantly on the material selection, deposition methods and deposition process parameters. Materials can be deposited in the form of thin film on a substrate by a variety of methods such as physical vapour deposition, chemical vapour deposition, wet-chemical processes such as sol-gel and electrochemical deposition and spray pyrolysis etc. To deposit stacked materials of different natures by precisely controlling their chemical composition, surface morphology, microstructure, and phase will be a challenge. [1]. It is believed that transition metal oxides are good candidates as electrode materials, because they have variation in oxide states which is suitable for effective redox charge transfer [2-4]. Non-noble oxides such as NiO, Co_3O_4, MnO_2 are very promising candidates for electrode materials in supercapacitors [5-12]. These oxides show specific capacitance varying between 100 and 400 F/g. However, the relatively low specific capacitance needs to be improved for supercapacitor application. Recent research is focused on increasing the specific capacitance of the oxides by introducing other oxides technology [13−14]. In this study, MnO_2, Co_3O_4 and MnO_2:Co_3O_4 stacked oxides as electrode materials were prepared by Sol-gel spin coat method. The physical and structural properties of the oxides were characterized. The capacitive characteristics of the stacked oxides as the active electrode materials for supercapacitors were also investigated by electrochemical characterizations.

II. EXPERIMENTAL

A. Sol-Gel Preparation

At first 0.02M solution of cobalt acetate [(CH3COO)2Co.4H2O] and manganese acetate [C4H6MnO4.4H2O] were prepared in a double distilled water and isopropyl alcohol. The prepared solution was stirred for 4 hours and then aged for 48 hours. Then prepared sol-gel is spin coated on steel substrate to obtain thin film electrodes.

Volume 4 Issue IV, April 2016
ISSN: 2321-9653
International Journal for Research in Applied Science & Engineering Technology (IJRASET)

B. Deposition Of The Films

Before deposition, the steel substrates were polished with zero grade polish paper and washed with double distilled water in an ultrasonic bath for 15 minute. To deposit the film by spin coat method, few drops of gel are placed on the steel substrate, which is then rotated at high speed (3000rpm) in order to spread the fluid by centrifugal force. The film thickness can be adjusted by varying the rotation speed, the rotation time, and the viscosity of the gel. After deposition, film was annealed at 900^0C under furnace. To deposit stacked thin films, first two layers of manganese acetate were deposited on steel substrate, then two layers of cobalt acetate were deposited and the film was annealed.

III. RESULT AND DISCUSSION

A. STRUCTURAL ANALYSIS BY XRD

Structural analysis was carried out by D2 PHASER diffractometer with steps one degree per minute using source CuKα1 with λ =1.54184Å. The 2θ angle is varied from 10^0 to 80^0. The fig.1 shows the XRD pattern for Co_3O_4, MnO_2 and MnO_2:Co_3O_4 stacked oxide thin films. XRD pattern exhibit crystalline nature with orthorhombic [15] and cubic phase [16] for MnO_2 and Co_3O_4 films respectively. The XRD pattern of MnO_2:Co_3O_4 stacked film shows dominating peaks of both oxides and two new peaks of MnO_2. It also shows small shift in angle 2θ hence shifting the lattice constants. The details of all the peaks and lattice constants are given table.1 and table.2 respectively. The lattice mismatches between pure and stacked films indicate significant variations occurred on the structures and properties of stacked thin film.

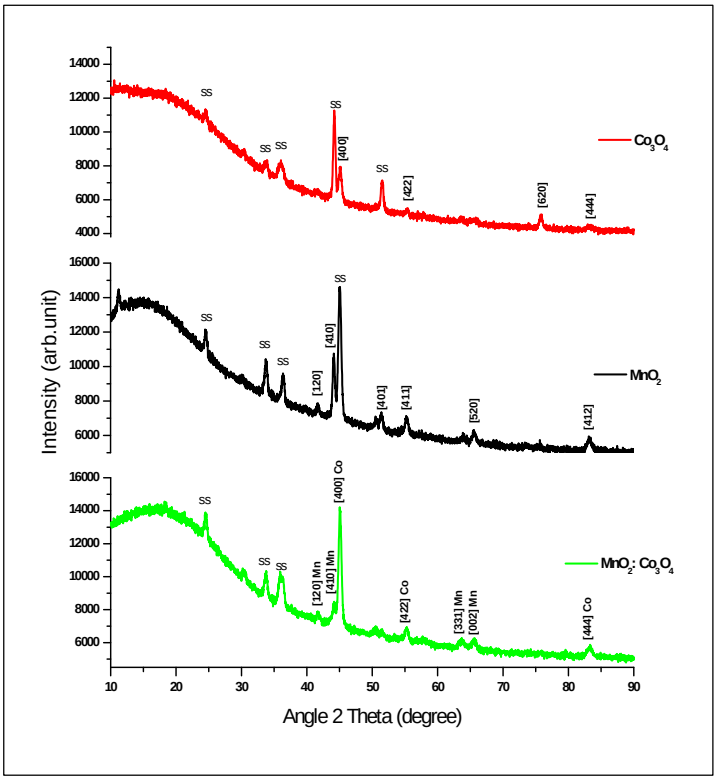

Fig. 1 XRD patterns of Co_3O_4, MnO_2 and MnO_2:Co_3O_4 stacked oxide thin films

Film	Plane [hkl]	Observed 'd'	Standard 'd'
Co_3O_4	[400]	2.030	2.021
	[422]	1.677	1.650
	[620]	1.265	1.278
	[444]	1.168	1.166

Volume 4 Issue IV, April 2016
ISSN: 2321-9653
International Journal for Research in Applied Science & Engineering Technology (IJRASET)

MnO_2	[120]	2.184	2.165
	[410]	2.070	2.065
	[401]	1.794	1.807
	[411]	1.679	1.672
	[520]	1.438	1.430
	[412]	1.172	1.172
MnO_2:Co_3O_4	[120]	2.166	2.166
	[410]	2.048	2.065
	[400]	2.012	2.021
	[422]	1.659	1.650
	[130]	1.460	1.465
	[002]	1.421	1.424
	[444]	1.159	1.166

Table. 1 standard interplanar spacing dhkl for the Planes of MnO_2, Co_3O_4 and MnO_2:Co_3O_4 stacked oxide thin films.

Film	Plane [hkl]	Lattice constant 'a'		Lattice constant 'b'		Lattice constant 'c'	
		Obs	Stand	Obs	Stand	Obs	Stand
MnO_2	[120]	9.363	9.322	4.493	4.453	2.855	2.848
	[410]						
	[411]						
MnO : Co_3O_4	[120]	8.880		4.332		2.841	
	[410]						
	[002]						
Co_3O_4	[400]	8.144	8.085	-	-	-	-
	[422]						
	[444]						
MnO : Co_3O_4	[400]	8.068					
	[422]						
	[444]						

Table. 2 Observed shift in lattice parameters for the corresponding Planes of MnO_2, Co_3O_4 and MnO_2:Co_3O_4 stacked oxide thin films.

B. Surface Morphology By SEM

The morphological features of the samples were investigated by Scanning Electron Microscopy (SEM) using a JEOL JSM-6360 instrument. From the SEM analysis it has been observed that the grain structure of both MnO_2 and Co_3O_4 films is tetragonal with smooth, well adherent and porous surface. As shown in fig. 2 (a) and (b) MnO_2 and Co_3O_4 thin films possess large grains uniformly distributed throughout the film surface, the average grain size calculated from the SEM images are around 500nm and 600nm respectively. From fig 2 (c), it is observed that, the grains are more equated with continuous grain boundary with decreased grain size

in the range 250nm, this indicates MnO_2: Co_3O_4 stacked thin film exhibit enhanced pore density and grain density which is major requirement in supercarpacitor.

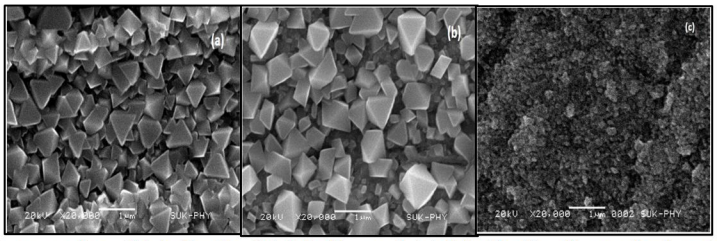

Figure. 2 SEM micrographs of (a) Co_3O_4 (b) MnO_2, and (c) MnO_2:Co_3O_4 stacked oxide thin films.

C. Electrochemical Analysis

All electrochemical parameters were studied by using CHI 680E 'Electrochemical Workstation, Instrument purchased from USA.

1) Cyclic Voltammetry: The supercapacitive properties of the MnO_2, Co_3O_4 and MnO_2: Co_3O_4 stacked electrodes were determined using cyclic voltammetry because this method provides valuable information on the charge-discharge behaviour of the electrodes. The measurements were performed with MnO_2, Co_3O_4 and MnO_2: Co_3O_4 stacked thin films as working electrode and platinum wire as counter electrode and SCE as a reference electrode in 0.1 M KOH electrolyte. Fig. 3 shows the cyclic voltammograms for all the electrodes with different potential windows at various scan rates 10, 20, 40, 60, 80 and 100mV/sec. From CV analysis, MnO_2, Co_3O_4 and MnO_2:Co_3O_4 stacked films showed maximum specific capacitance of 440 F/g, 530 F/g and 600 F/g respectively at 10mV/s scan rate.

In all CV curves, reduction and oxidation peaks are visible. This indicates that the electrochemical capacitance of the electrodes mainly results from pseudocapacitance [17]. All CV graphs demonstrate that the current response increased with the scan rate. Furthermore, as the scan rate increased above 10 mVs^{-1}, the voltammograms 'window' tends to tilt toward the vertical axis, thereby becoming a quasi-rectangle. This result indicates the dominance of the double layer formation in the energy storage process at lower scan rates [18].

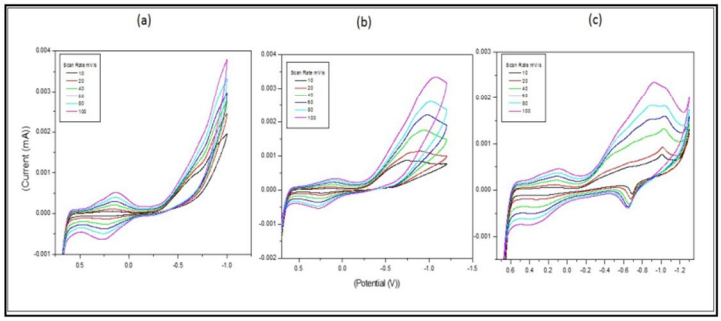

Figure.3 Cyclic Voltammograms of (a) MnO_2, (b) Co_3O_4 and (c) MnO_2:Co_3O_4 stacked electrodes

Comparing the voltammograms of the MnO_2, Co_3O_4 and MnO_2: Co_3O_4 electrodes, it can be observed that MnO_2:Co_3O_4 stacked electrode has a broader voltammogram area, this reveals the better cycle reversibility and higher electric double-layer capacitance stability during the charge and discharge processes compared with the pure electrodes. Ultimately, these effects correspond to a higher specific capacitance for the stacked electrode [18]. The details of specific capacitance are given in table. 3.

Scan Rate(mV/s)	Specific Capacitance (F/g)		
	MnO_2	Co_3O_4	MnO_2:Co_3O_4
100	118	165	218
80	116	179	235
60	131	202	262
40	157	247	300
20	244	342	372
10	447	530	600

Volume 4 Issue IV, April 2016
ISSN: 2321-9653
International Journal for Research in Applied Science & Engineering Technology (IJRASET)

Table. 3 Specific capacitance at different scan rates of MnO_2, Co_3O_4 and MnO_2:Co_3O_4 Stacked oxide thin film electrodes.

All electrodes showed a common trend of decreasing specific capacitance values against an increasing scan rate. It is well known that for very low scan rates, the specific capacitance values are higher because the ions have a much longer time to penetrate and reside in all the available electrode pores and form electric double layers, which are needed to generate higher capacitance. Despite this common trend, the MnO_2: Co_3O_4 stacked electrode displays higher specific capacitance values throughout the whole scan region [18], clearly indicating its superiority over the pure electrodes. This is in good agreement with the values shown in table. 3.

2) STABILITY TEST: Since the MnO_2:Co_3O_4 stacked film gave the highest capacitance, we investigated the stability of the film for longer votammograms upto 1000 cycles at the scan rate of 500mVs^{-1} in 0.1M KOH electrolyte lasting about 3hour, is shown in fig. 4. There are no major changes between CV's and the total area enclosed by both curves, are probably similar to each other. 75% stability is retained after 1000th cycle, the value of specific capacitance is decreased by a comparably small amount which may be due to detatchment during early charging/discharging cycles in the electrolyte [19].

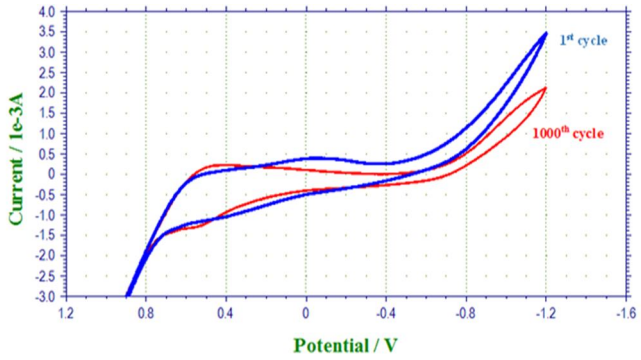

Figure.4 CV curves of (a) MnO_2, (b) Co_3O_4 and (c) MnO_2: Co_3O_4 stacked electrodes at 1st and 1000th cycle at 500mV/s scan rate.

3) CHRONOPOTENTIOMETRY : Chronopotentiometric charge-discharge is the most reliable and accurate method for evaluating super-capacitor properties of electrodes. Typical charging and discharging curves for MnO_2, Co_3O_4 and MnO_2:Co_3O_4 stacked electrodes were measured between the voltage range of -1 to 1V at a current density of 1, 2 and 3mA cm^2 respectively in 0.1 M KOH electro-lyte as shown in figure. 5. It is observed that charging-discharging time are almost same but there is a difference in potential range, the maximum potential is observed for MnO_2:Co_3O_4 stacked oxide thin film.

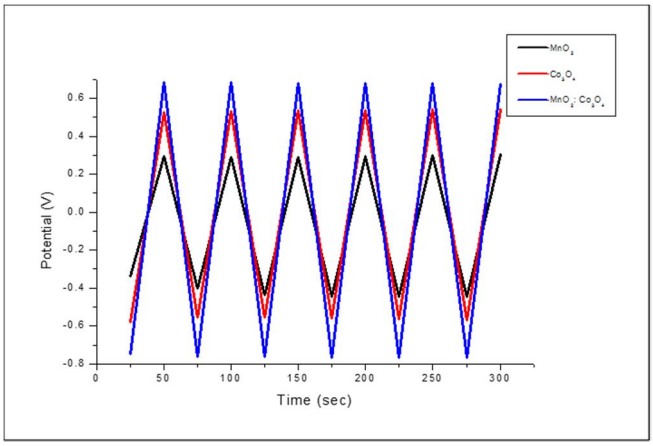

$$\text{Specific energy S.E} = \frac{V \times I_d \times T_d}{W} \quad (1)$$

$$\text{Specific energy S.P} = \frac{V \times I_d}{W}, \text{ and} \quad (2)$$

$$\text{Coulombic efficiency } \eta \ (\%) = \frac{T_d}{T_c} \times 100 \quad (3)$$

Fig. 5 Charge-discharge curves of MnO_2, Co_3O_4 and MnO_2:Co_3O_4 stacked oxide electrodes From CP, the supercapacitive parameters such as specific energy, specific power and coulombic efficiency were calculated using,

Where, I_d and T_d are the discharge current and discharge time, respectively. The W is the mass of the film. From calculations,
The MnO_2, Co_3O_4 and MnO_2:Co_3O_4 stacked films exhibited specific energy 29.13 Wh/kg, 72.22 Wh/kg, 141.66 Wh/kg respectively and specific power 20KW/kg, 52.00 KW/kg, 68.00 KW/kg respectively. The columbic efficiency for all the electrodes was fond to be

100%.

4) Electrochemical Impedance Spectroscopy (EIS): The EIS data expressed as Nyquist plots over the frequency range of 1Hz to 10^5Hz for the MnO_2, Co_3O_4 and MnO_2:Co_3O_4 stacked electrodes are given in figure. 6. The inset figure, clearly shows the small semicircle, Waburg diffusion line (straight line with a slope of approximately 45°) and capacitive line (straight lines sharply increasing at the low-frequency region). A relatively small semicircle in the high frequency region represents the dominant resistive nature of the supercapacitor system consisting of electrode/electrolyte/current-collector. The beginning of the semicircle line (left-intercept of Z'' at the Z' axis) represents the resistance (R_s) of the electrolyte in contact with the current collector and electrode. The termination of the semicircle line (right-intercept of Z'' at the Z' axis) represents the internal resistance (R_p) of the electrode. The diameter of the semicircle (R_p-R_s) is equal to the ESR value. The values of R_s, R_p and ESR for all the films determined from the data in figure.6 are listed in table. 4.

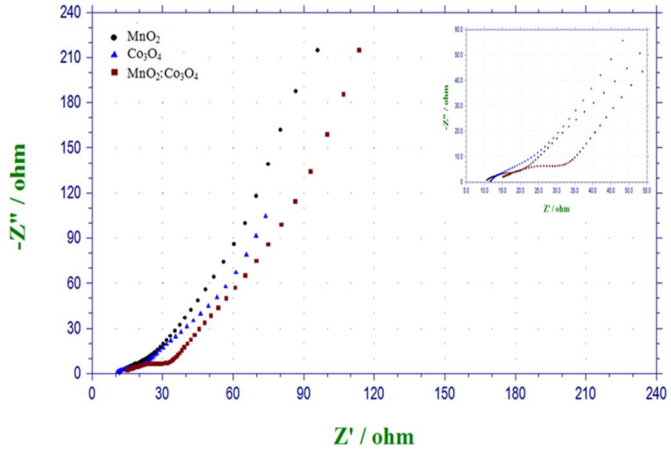

Figure. 6 Nyquist plots for the MnO_2, Co_3O_4 and MnO_2: Co_3O_4 stacked oxide thin films.

Films	Rs (Ω)	Rp (Ω)	ESR (Ω)	fk (Hz)	Rk (Ω)
MnO_2	14	17	3	9.83	55
Co_3O_4	10.6	13.6	3	3.74	49
MnO_2: Co_3O_4	15	17.5	2.5	8.07	60

Table. 4 Values of R_s, R_p, ESR, F_k and R_k for MnO_2, Co_3O_4 and MnO_2:Co_3O_4 stacked oxide thin films.

Waburg diffusion line in the middle frequency region represents the combination of resistive and capacitive behaviours of the ions penetrating into the electrode pores. The length, slope and position of this segment appear to be good as compared to both pure films [20].

A capacitive line represents the dominance of capacitive behaviour from the formation of ionic and electronic charges of the electric double layer system at the micropore surfaces at this frequency, the ions can more easily diffuse into the micropores [20-22]. The initiation point of this capacitive line corresponds to the knee frequency (f_k), and its corresponding resistance (R_k) is given by Z'_k. The values of f_k and R_k are given in table. 4. Furthermore, the line for the MnO_2: Co_3O_4 stacked electrodes leans towards the vertical Z" axis indicating that, it has a better capacitive performance. Similarly as observed from the results shown in table. 4, the MnO_2:Co_3O_4 stacked electrode has minimum ESR value as compared to pure electrodes indicating again a good capacitive behaviour.

IV. CONCLUSION

This study shows successful synthesis of MnO_2, Co_3O_4 and MnO_2:Co_3O_4 stacked oxide thin films as confirmed by the different characterizations such as XRD, SEM, CV, Stability, Chronopotentiometry and EIS. XRD revealed the formation of metal oxides which are crystalline in nature, the XRD pattern of stacked film include dominating peaks of both metal oxides. The lattice mismatches between pure and stacked films indicate significant variations occurred on the structures and properties of stacked thin film to some extent. The

Volume 4 Issue IV, April 2016
ISSN: 2321-9653

SEM images clearly indicated the enhanced porous nature of MnO_2:Co_3O_4 stacked oxide as compared to pure thin films. Cyclic Voltammetry, Electrochemical Impedance Spectroscopy and Charge-discharge techniques revealed that MnO_2:Co_3O_4 stacked oxide electrode exhibited good electrochemical behaviour. It has been also observed that value of specific capacitance is more and ESR is less for stacked electrode as compared to pure electrodes. The stacked electrode demonstrated high stability with no significant changes over 1000 cycles.

V. ACKNOWLEDGMENT

Authors are grateful to the U.G.C, New Delhi for financial support through the Major Research Project F No. 42-123/2013(SR).

REFERENCES

[1] Dongfang Yang, Industrial Materials Institute, National Research Council Canada, www. intechopen.com
[2] A. K. Shukla, S. Sampath, K. Vijayamohanan, Current Science. 2000, 79, 1656.
[3] P. J. Hall, M. Mirzaeian, S. I. Fletcher, F. B. Sillars, A. J. R. Rennie, G. O. Shitta-Bey, G, Energy & Environmental Science. 2010, 3, 1238.
[4] P. Simon, Y. Gogotsi, Nature Materials. 2008, 7, 845.
[5] V. Srinivasan, J.W. Weidner. J Electrochem Soc, 2000, 147, 880.
[6] W.U Meng-qiang, Jia-hui, Shu-ren, et al. J Power Sources, 2006, 159:365.
[7] C. Lin, J. A. Ritter, B. N. Popov, J Electrochem Soc, 1998, 145, 4097.
[8] J. N. Broughton, J.Brett, Electrochim Acta, 2004, 49, 4439.
[9] Luo S L, J. Electrochem Soc, 2006, 153, A1317.
[10] S. Devaraj, N. Munichandraiah, J. Electrochem Soc, 2007, 154, A80.
[11] A. Zolfaghari, F. Ataherian, M. Ghaemi, et al. Electrochimica Acta, 2007, 52, 2806−2814.
[12] Zhang, Zhi-an, Lai Yan-qing, Li Jie, Liu Ye-xiang J. Cent.SouthUniv.Technol.2007,0638−05DOI:10.1007/11771− 007−0122−0
[13] W. Yong, Z. Xiao, J. Electrochimica Acta, 2004, 49, 1957−1962.
[14] S. L. Kuo, J. F. Lee, N. L. Wu, J Electrochem Soc, 2007, 154, A34−A38. JCPDS: 82-2169 JCPDS: 78-1969
[15] A. D. Jagdale, V. S. Jamadade, Electromica Acta, 2012 78, 92-97
[16] R. Farma, M. Deraman1, Awitdrus, I.A. Talib1, R. Omar1, J.G. Manjunatha Int. J. Electrochem. Sci., 2013, 257 – 273.
[17] W.C. Chen, T.C. Wen and H. Teng, Electrochim. Acta, 48 (2003) 641.
[18] F. Rafik, H. Guolous, R. Gallay, A. Crausaz and A. Berthon, J. Power Source, 165, 928.
[19] Y.R. Nian and H. Teng, J. Electroanal. Chem., 540, 2003, 119.
[20] J. Gamby, P.L. Taberna, P. Simon, J.F. Fauvarque and M. Chesneau, J. Power Sources, 101, 2001, 109.

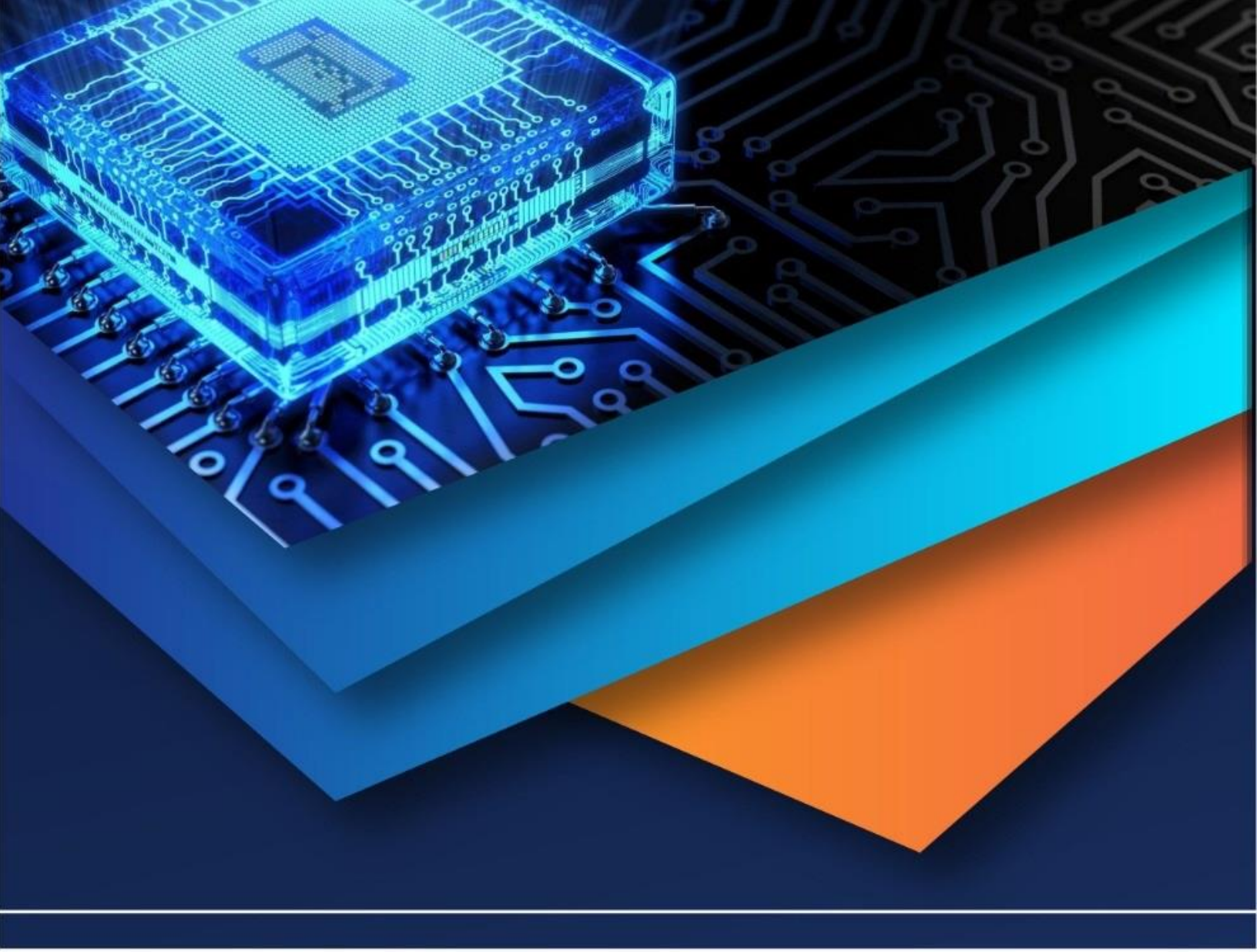

10.22214/IJRASET

45.98

IMPACT FACTOR: 7.129

IMPACT FACTOR: 7.429

INTERNATIONAL JOURNAL FOR RESEARCH

IN APPLIED SCIENCE & ENGINEERING TECHNOLOGY